

P1.26 APPLICATION OF THE NASA A-TRAIN TO EVALUATE CLOUDS SIMULATED BY THE WEATHER RESEARCH AND FORECAST MODEL

¹Andrew L. Molthan*, ²Gary J. Jedlovec and ²William M. Lapenta

¹Department of Atmospheric Science, University of Alabama Huntsville

²Short-Term Prediction Research and Transition (SPoRT) Center, NASA/MSFC

1. Introduction

On the temporal and spatial scales of regional weather, accurate forecasts of cloud cover are required to predict the diurnal temperature cycle and probability of precipitation. Clouds and precipitation disrupt transportation, or in severe cases may contribute to flooding, property damage or agricultural losses. Many of these problems are alleviated through risk mitigation strategies, enhanced by accurate weather forecasts in the form of watches and advisories. Numerical models assist with the issuance of these forecast products. Gains in forecasting will come from improved simulation of clouds and their microphysical processes, achieved through steady increases in computer resources and forecast models that operate at cloud resolving resolution.

2. Background

High resolution forecast models are transitioning to the use of bulk water parameterizations that explicitly forecast the evolution of clouds and precipitation. Investment in the NASA Afternoon Train (or A-Train) of polar-orbiting, Earth observing satellites provides an opportunity to observe cloud properties, which provide data for the validation and improvement of simulated clouds within high resolution models. Specifically, the launch of the CloudSat Cloud Profiling Radar has returned two-dimensional

curtains of cloud reflectivity that may be compared to their model simulations through use of a radiative transfer model.

2.1 Single-Moment Microphysics Schemes

The cloud life cycle is simulated by distributing water mass among multiple hydrometeor classes in a bulk water parameterization scheme. Although the numbers of classes vary among schemes, each is responsible for the representation of physical processes through formulas describing their sources and sinks. Model grid points contain the mixing ratio of each hydrometeor class, yet the physical processes of terminal fall speed, geometric sweep out and collision efficiency require knowledge of particle sizes. This requirement is met by assuming a particle size distribution relating the mixing ratio to the number of particles within a given size interval. These functions are smooth and continuous, often prescribed as an inverse-exponential form following from an analysis of raindrop sizes performed by Marshall and Palmer (1948). The inverse exponential distribution determines the number concentration of a particular diameter and is dependent upon an intercept and slope parameter. The slope parameter is a function of the particle density, an intercept parameter and the mixing ratio. Given a constant mixing ratio, reducing (increasing) the intercept parameter increases (decreases) the mean particle diameter.

Currently, operational schemes are limited to “single-moment” routines that include prognostic equations for the mixing ratios of a limited number of hydrometeor

Corresponding author address: Andrew L. Molthan
Department of Atmospheric Science
University of Alabama Huntsville
320 Sparkman Drive, Huntsville, AL, 35805
email: andrew.molthan@nssc.uah.edu

classes. Other “double-moment” schemes predict both the mixing ratio and number concentrations of various size categories but will not be discussed here. Two single-moment, six-class bulk water parameterizations are of particular interest: the NASA Goddard Cumulus Ensemble (Tao and Simpson 1993, Tao et al. 2003 and GSFC6 hereafter) and the Weather Research and Forecasting Model (WRF) Single-Moment (Hong et al. 2006 and Hong et al. 2004, WSM6 hereafter) microphysics schemes.

2.2 The Weather Research and Forecast (WRF) Model

Bulk water microphysics schemes are currently utilized in operational, high-resolution forecasts generated by the Weather Research and Forecast (WRF) Model (Skamarock 2007). This model is used extensively by federal agencies responsible for public safety: the National Centers for Environmental Prediction (NCEP), the National Severe Storms Laboratory (NSSL), and individual National Weather Service offices produce forecasts using the WRF model framework. The WRF model can be initialized off of other model forecasts or may generate fresh initial conditions through variational data assimilation techniques. The model operates in a non-hydrostatic mode to accommodate mesoscale simulations and provides a battery of parameterizations for land surface, boundary layer, radiation, and cumulus processes. Tao et al. (2007) have incorporated the Goddard microphysics scheme in the WRF model framework, while a variety of other schemes are available for comparison.

2.3 CloudSat Cloud Profiling Radar

The CloudSat Cloud Profiling Radar (CPR) was launched in 2006 and builds on the heritage of ground-based cloud radars, using a

94 GHz frequency to produce two-dimensional curtains of cloud reflectivity (Stephens et al. 2002). CloudSat samples clouds slightly off of the nadir point, providing a 1.7 km along track and 1.4 km across track resolution, with reflectivity resampled to a vertical resolution of 240 m (L’Ecuyer, personal communication). The radar system has a minimum detection threshold of -28 dBZ, but has difficulty sampling in the lowest 1 km of the atmosphere due to cluttering from the Earth’s surface. A quality control mask has been developed to eliminate noisy signals from true cloud returns (Wang and Sassen 2007). In ground-based applications, radars similar to CloudSat have been used to observe the “seeder-feeder” precipitation process in an extratropical cyclone (Syrett et al. 1995), determine cloud layering statistics (Hogan 2000), and cloud base and top altitudes (Wang and Sassen 2001). Although CloudSat may have difficulty detecting thin cirrus and will attenuate strongly in areas of moderate or heavy precipitation, the bulk of the radar profile reveals the characteristics of clouds in the mixed phase region responsible for many microphysical processes and the generation of precipitation.

2.4 QuickBeam Radiative Transfer Model

A radiative transfer model (QuickBeam) has been developed for the simulation of CloudSat reflectivity profiles, given a vertical profile of altitude, pressure, temperature and hydrometeor mixing ratios (Haynes et al. 2007). QuickBeam is used here to produce reflectivity profiles from clouds simulated within a high-resolution WRF forecast. The QuickBeam code has been modified slightly to include particle size distribution characteristics unique to the WSM6 microphysics scheme: the determination of a mean cloud ice crystal size as a function of mixing ratio, and the

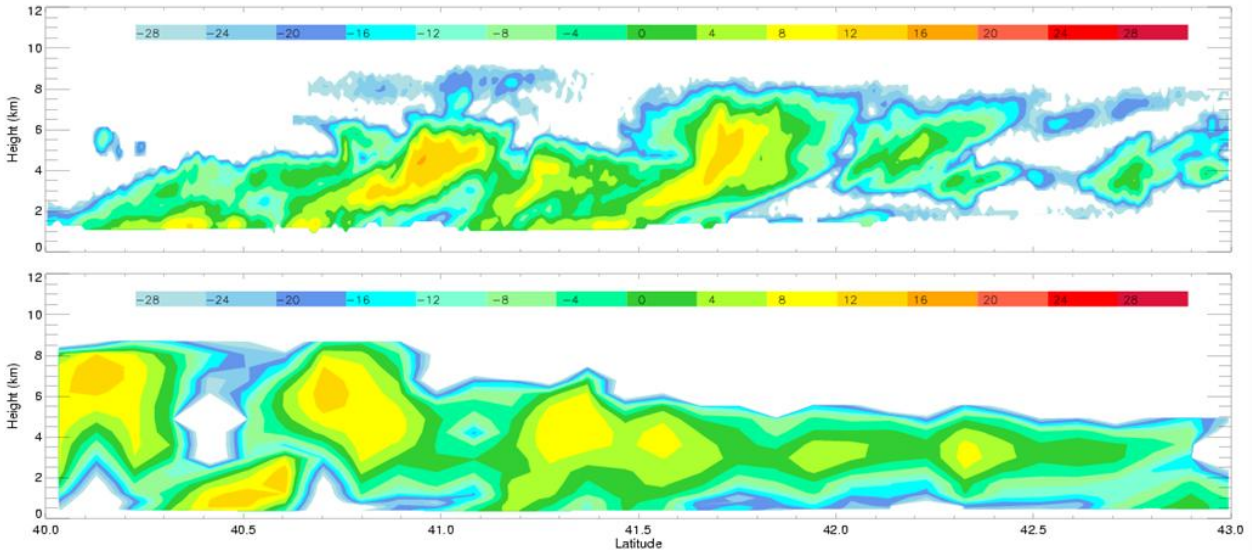


Figure 1. [Top] CloudSat Cloud Profiling Radar reflectivity (dBZ) observations of light to moderate, precipitating snow bands observed on 1 March 2007 in Eastern Nebraska and Western Iowa. [Bottom] QuickBeam simulated reflectivity based on WRF cloud profiles extracted from an operational NSSL forecast, taken from grid points that were nearest neighbors to the CloudSat nadir track.

temperature dependence of the snow distribution intercept parameter (Hong and Lim 2006). An example comparison of CloudSat observations and reflectivity obtained through QuickBeam is shown in Figure 1.

2.5 Remote Sensing Strategies for Validating Microphysics Schemes

Due to the frequent use of bulk water schemes when investigating cloud processes, and a future reliance upon them for high-resolution operational forecasts, Lang et al. (2007) emphasize a need to identify scheme biases and necessary adjustments. Contoured frequency with altitude diagrams (CFADs, Yuter and Houze 1995) are often used to provide a graphical representation of the radar reflectivity distribution along a constant altitude. Although a single frequency radar signal cannot separate the reflectivity into contributions from specific hydrometeor types, inferences may be made by examining the vertical distribution of mixing ratios as

simulated by the model in comparison to the location of modeled and observed differences. These inferences may be validated through an experimental design that modifies a specific microphysical process and identifies changes that tune the model toward observations.

3. Methodology

The Weather Research and Forecast (WRF) Model (Skamarock 2005) was used in an operational mode and at high resolution in order to explicitly simulate the evolution of clouds and precipitation. This model is currently being run at the National Severe Storms Laboratory (NSSL) to supplement other objective forecast tools available to the Storm Prediction Center and National Weather Service forecast offices. Daily forecasts produced by NSSL utilize the MYJ boundary layer and turbulence, the WRF six-class bulk water microphysics (WSM6), the Rapid Radiative Transfer Model (RRTM) for longwave radiation, and the the Dudhia shortwave radiation schemes as well as a

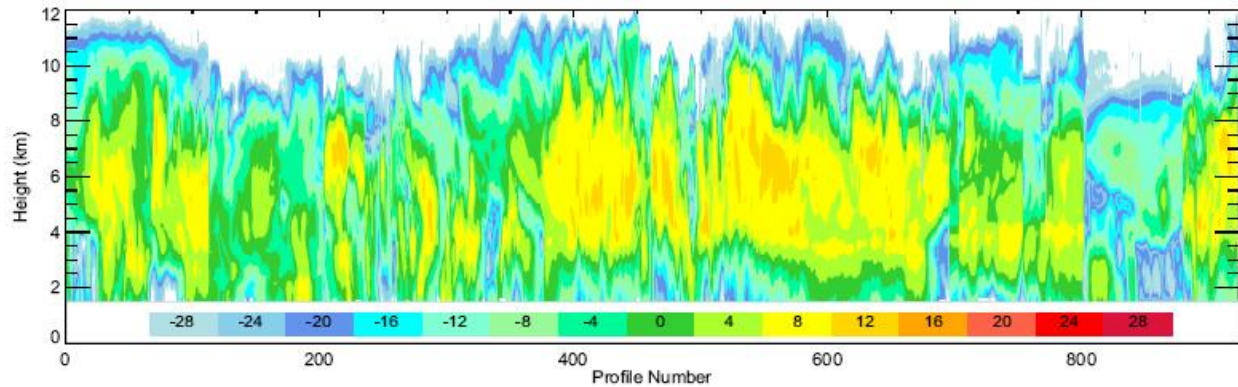


Figure 2. Combined reflectivity profiles (dBZ) for deep frontal and convective clouds based on CloudSat 2B-CLDCLASS profile classification and 2B-GEOPROF reflectivity accumulated throughout October 2006 within the Central United States.

positive-definite advection of moisture (NSSL 2007). The NSSL forecasts use 35 vertical levels, a 24-second time step and a horizontal resolution of 4 km with coverage over most of the continental United States. The NSSL selection of parameterizations was adhered to in this study to make comparisons between observed clouds and those simulated by an operational model. The single-moment bulk microphysics scheme was varied to compare the representation of cloud types in the GSFC6 and WSM6 forecasts to observations from CloudSat.

The QuickBeam radar simulator was used to convert cloudy WRF profiles into equivalent CloudSat reflectivity. Each WRF

simulation was analyzed to locate a section with comparable cloud types of interest: deep convective or stratiform profiles. These profiles were composited and compared to observations of deep convective and stratiform cloud profiles obtained by CloudSat.

4. Model Simulations and Results

Two extratropical cyclones were simulated with six-class microphysics, producing output mixing ratios of water vapor, cloud ice, cloud water, rain, snow and graupel. Both cyclones traveled through the Central Plains, producing varying types of precipitation across several states. The cyclone of 22 February 2007 brought light to moderate snow to the states of Iowa and Minnesota, with snowfall continuing northward into the central Canadian provinces. This storm was sampled by CloudSat during an ascending pass around 19 UTC, with moderate snow bands represented by 8-12 dBZ reflectivity maxima extending 3-4 km AGL to just above the surface. On the synoptic scale, this snowfall event and cloud shield occurred in a region of isentropic ascent and warm air advection. Cold season precipitation forecasts are a current target of weather prediction research (Ralph et al. 2005), and this case is used to compare WRF representation of winter precipitation profiles

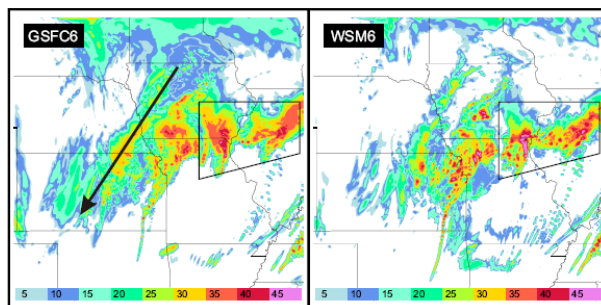


Figure 3. Simulated composite WSR-88D reflectivity (dBZ) at 09 UTC on 1 March 2007. A polygon encompasses WRF profiles sampled to represent convective cloud profiles. The CloudSat flight track used in Figure 1 is represented by an arrow.

to a known case of CloudSat snowing profile observations.

One week later, another midlatitude cyclone produced a narrow band of snow in the Central Plains, thunderstorms to the Midwest and severe weather to the Gulf Coast on 1 March 2007. CloudSat sampled light to moderate snow bands, and a particularly skillful NSSL WRF forecast allowed for a direct comparison between observed and simulated CloudSat reflectivity (Figure 1). The WRF model appears capable of producing cloud top altitude and layering characteristics similar to observations, as well as banded precipitation structures with reasonable reflectivity maxima and altitudes. These similarities provide a justification for continued use of CloudSat and QuickBeam in model validation and improvement. The 1 March 2007 simulation produced two clusters of active convection, which was used in a first comparison to CloudSat convective cloud profiles. The limited spatial and temporal coverage of CloudSat required an aggregation of several deep convective profiles for comparison.

4.1 Comparisons of Convective Profiles

The CloudSat Data Processing Center provides a classification product that categorizes radar profiles into nine types based on reflectivity values, altitude and temperature (2B-CLDCLASS, Wang and Sassen 2007). Cloud classification data were used to accumulate all radar profiles categorized as deep precipitating clouds (DP) for the month of October 2006 that were observed in the Great Plains and Midwest (Figure 2). In addition, given that convective clouds can have a wide range of cloud top heights that depend on varying equilibrium levels and buoyancy, the CloudSat DP cloud profiles were trimmed to only include those with cloud tops in the range of 10-12 km, with cloud top determined by the altitude of the

highest, cloud-confident radar return. CloudSat profiles meeting these criteria were combined into a contoured frequency with altitude diagram to visualize the distribution of reflectivity with altitude.

The CloudSat CFAD contains a mode of low reflectivity at high altitude, generated by cirriform clouds associated with active and decaying convection. The range and mode of reflectivity between 10 and 12 km are a result of the varying cloud top altitudes within the CloudSat sample (Figure 4). Otherwise, these profiles have a mode of 8-16 dBZ in the 2-7 km layer associated with the formation of snow crystals and graupel, precursors to surface precipitation. The broadening of the reflectivity distribution below 2 km is due to attenuation in some convective regions, as well as observations of the higher reflectivity of precipitation that is likely reaching the surface.

Model vertical profiles were extracted for a small section of active convection that occurred in the 1 March 2007 simulations (Figure 3) to compare observed convective clouds and their modeled counterparts. These profiles were converted to CloudSat reflectivity through use of the QuickBeam simulator and combined into CFAD images for comparison (Figure 4). Differences are noted through subjective comparisons of the reflectivity mode in CloudSat observations and the two six-class schemes. Both schemes produce reflectivity modes in the 4 to 8 km layer, similar to CloudSat observations. The WSM6 scheme produces greater maximum reflectivity up to 8 km AGL, although these values are still 4 to 8 dBZ less than observed. Both the GSFC6 and WSM6 schemes underestimate the reflectivity mode in the 4 to 8 km layer. This difference may be attributable to errors in the size distribution or the forecast mixing ratios of hydrometeor constituents, or both. Nearer to the surface, modeled and observed CFADs show a broadened reflectivity distribution due to

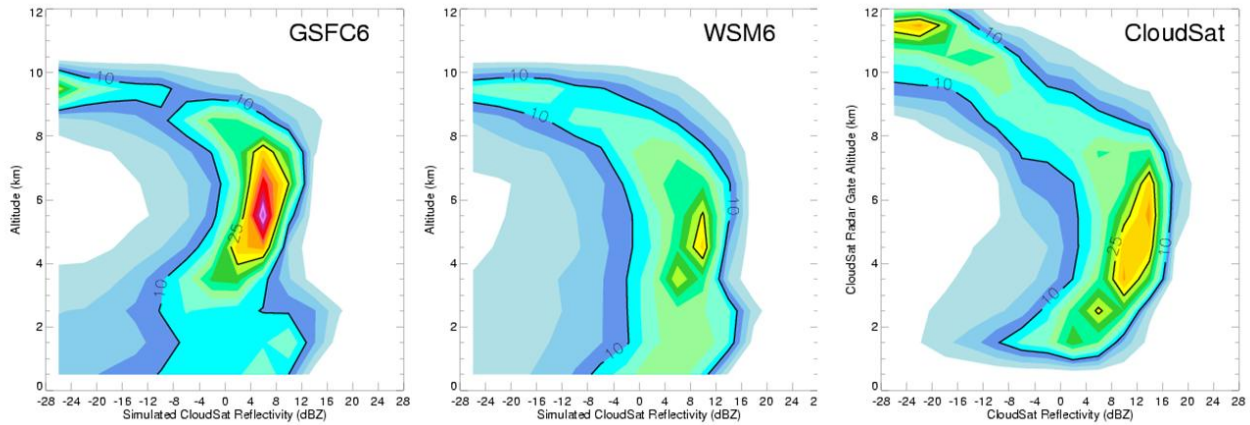


Figure 4. Contoured frequency with altitude diagrams (%) of observed and simulated CPR reflectivity for observed and modeled convective profiles. Reflectivity is simulated with QuickBeam using the subset (polygon) in Figure 3. CloudSat reflectivity is composed of profiles in Figure 2. Shading interval is 2.5% with contours of 10% and 25% provided for reference.

variations in the intensity of precipitation and attenuation of the radar signal.

4.2 Comparisons of Stratiform Profiles

CloudSat sampled clouds associated with warm frontal ascent during the passage of a midlatitude cyclone on 22 February 2007. Although there are repeated, isolated cores of enhanced reflectivity, weak vertical velocities drive the precipitation processes. Light to moderate snowfall limits the attenuation of the CloudSat radar signal, which provides additional detail down to the lowest cloud-

confident radar gates (Figure 5). The CloudSat flight track is sampled from 45 to 55 degrees latitude with reflectivity profiles merged into a contoured frequency with altitude diagram. Simulations were performed with the WRF model, and a polygon was selected to represent comparable precipitating cloud profiles. Although the actual CloudSat observations extend outside the model domain, the comparison of interest involves WRF precipitating and actual precipitating profiles. CloudSat observations continue to be relatively homogeneous into the Canadian provinces and were retained for comparison.

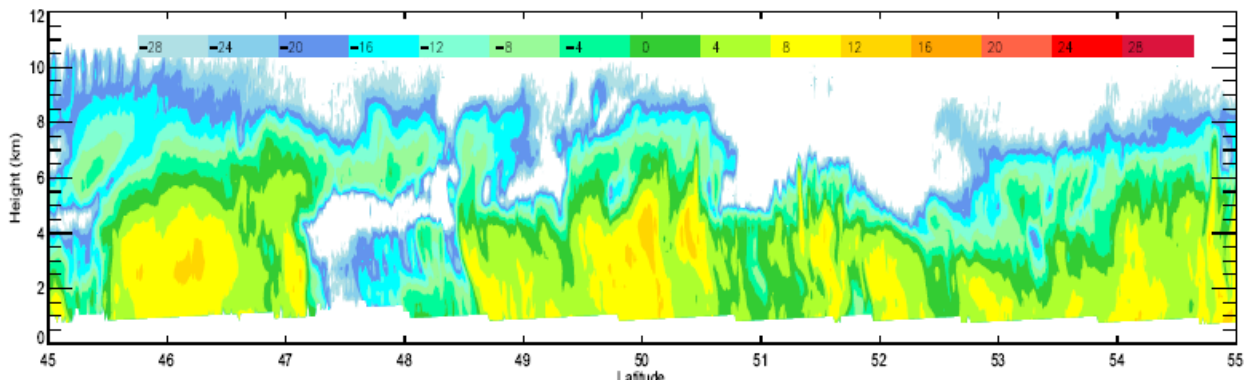


Figure 5. CloudSat reflectivity (dBZ) from 45 to 55N degrees latitude along the orbit segment (arrow) in Figure 6. This includes precipitating clouds outside the model domain in Figure 6.

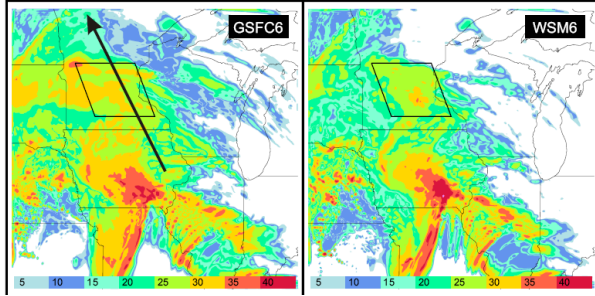


Figure 6. Simulated composite WSR-88D reflectivity (dBZ) at 19 UTC on 22 February 2007. A polygon encompasses WRF profiles sampled to represent stratiform precipitation. The CloudSat track in Figure 5 is shown with an arrow.

Similar to the convective CloudSat CFAD, the stratiform case retains a high altitude reflectivity mode that is caused by the presence of cirriform clouds composed of smaller ice crystals. In this case, the separation of the upper level cloud from the stratiform section suggests that the upper layer of cloud cover has been transported into the scene from another portion of the cyclone. It is interesting to observe some vertically oriented streaks of reflectivity maxima, possibly related to a seeder-feeder process in some portions of the cross section. The CloudSat reflectivity distribution is broadened

around 6 km AGL due to the variability of cloud top altitudes in the stratiform region and the altitude of individual reflectivity maxima. Nearer to the surface, the CFAD displays a mode of 4-12 dBZ, consistent with cross section segments and surface observations that indicate precipitation in the form of light to moderate snowfall.

Modeled cloud profiles were converted to CloudSat reflectivity through use of the QuickBeam simulator and once again aggregated into CFADs for comparison. The GSFC6 and WSM6 schemes both produce a reflectivity mode in the 2 to 4 km AGL range, although CloudSat frequencies are reduced by variability along the single cross section. The GSFC6 scheme produces a high altitude mode from cloud ice crystals, while the WSM6 CFAD suggests a lower cloud top altitude. Cloud top heights estimated by the WRF post-processor system display smaller variations of cloud top properties than are suggested by these CFAD comparisons. The WSM6 monodisperse ice crystal formulation may be creating high numbers of small crystals that do not produce a significant 94 GHz reflectivity, while the post-processor defines clouds through mixing ratio thresholds. These

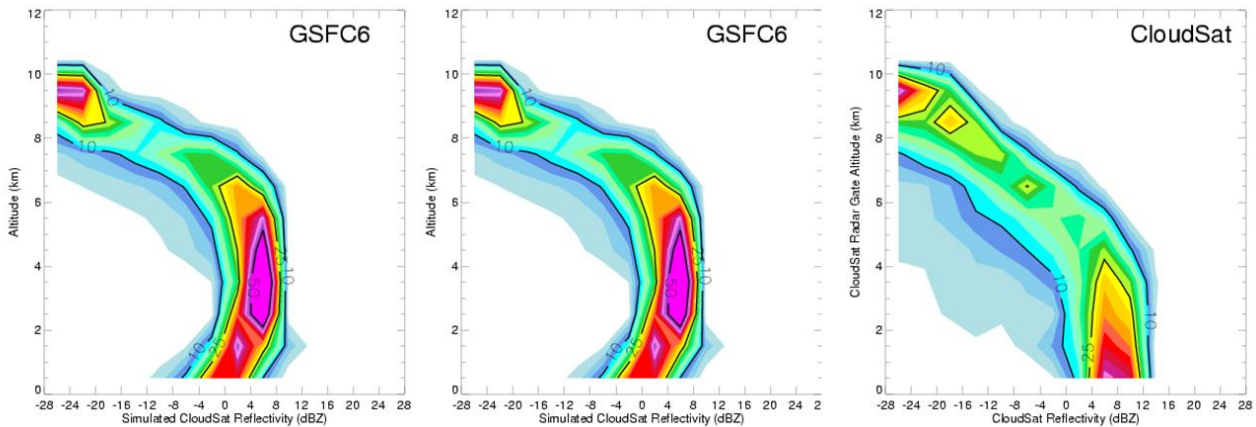


Figure 7. Contoured frequency with altitude diagrams (%) of observed and simulated CPR reflectivity for stratiform precipitation profiles. Model reflectivity is simulated with QuickBeam using the subset (polygon) in Figure 6. CloudSat reflectivity is composed of profiles in Figure 5. Shading interval is 2.5% with contours of 10%, 25% and 50% provided for reference.

differences warrant further investigation. In the lowest 4 km AGL, the WSM6 scheme generates maximum reflectivity values and frequencies similar to CloudSat, although reflectivity decreases nearest the surface. The GSFC6 scheme reflectivity is lower than WSM6, and the GSFC6 mode of 0 to 8 dBZ extends to a greater altitude. These differences are attributable to the mean profiles of graupel and snow. The GSFC6 scheme produced more than twice as much snow as the WSM6 run, where graupel was the dominant hydrometeor type. The WSM6 graupel mixing ratios contribute to larger reflectivity, while GSFC6 snow production aloft maintains a reflectivity of 0 to 8 dBZ to an altitude of 6 km AGL. These microphysical differences are a byproduct of the varied assumptions among the schemes. The WSM6 scheme includes additional parameterizations based on temperature, notably the inclusion of a snow distribution intercept parameter that is allowed to vary. This variation affects the mean size of snow crystals as well as the statistical representation of sources and sinks. These variations contribute to uncertainty in high resolution forecasts that can be alleviated through additional case studies and modifications that bring modeled clouds in line with CloudSat observations.

5. Conclusions and Summary

Four model simulations were performed for two midlatitude cyclones traversing the central United States during February and March 2007. Each pair of simulations compared model representations of clouds generated through six-class, single-moment bulk water microphysics schemes producing profiles of water vapor, cloud water, cloud ice, rain, snow and graupel. Analysis strategies were developed to compare CloudSat Cloud Profiling Radar

observations of real clouds to those produced in a high resolution forecast model.

Hydrometeor profiles were developed from a cluster of convection in Illinois. Variations in microphysical assumptions manifest in CFAD diagrams through variations in the range of simulated CloudSat reflectivity, the altitude and extent of the reflectivity mode, and forecast precipitation totals. Neither scheme produces an exact match to observations, demonstrating the need for additional forecast comparisons and improvements, coupled with validation of surface precipitation and other forecast parameters.

6. Acknowledgements

This work was performed in parallel with research sponsored by the NASA Short-Term Prediction Research and Transition (SPoRT) Center. The QuickBeam Radar Simulator was developed by John Haynes of Colorado State University. CloudSat data were obtained from the CloudSat Data Processing Center. The author benefitted from interaction with Drs. Wei-Kuo Tao and Toshi Matsui during discussions involving the Goddard Cumulus Ensemble bulk water microphysics scheme and the utility of a CloudSat simulator.

7. References

- Haynes, J.M., R.T. Marchand, Z. Luo, A. Bodas-Salcedo, and G.L. Stephens, 2007: A multi-purpose radar simulation package: QuickBeam. *Bull. Amer. Meteor. Soc.*, **88**, 1723-1727.
- Hogan, R. J. and A. J. Illingworth, 2000: Deriving cloud overlap statistics from radar. *Q. J. R. Meteor. Soc.*, **126**, 2903-2909.
- Hong, S-Y and J-O J. Lim, 2006: The WRF Single-Moment 6-Class Microphysics Scheme

(WSM6). *J. Korean Meteor. Soc.*, **42**, 129-151.

Lang, S., W.-K. Tao, R. Cifelli, W. Olson, J. Halverson, S. Rutledge and J. Simpson, 2007: Improving Simulations of Convective Systems from TRMM LBA: Easterly and Westerly Regimes. *J. Atmos. Sci.*, **64**, 1141-1164.

Mace, G. cited 2007: Level 2 GEOPROF Product Process Description and Interface Control Document Version 3.0. [Available online at http://www.cloudsat.cira.colostate.edu/ICD/2B-GEOPROF/2B-GEOPROF_PDICD_3.0.pdf]

National Severe Storms Laboratory, cited 2007: NSSL Real Time WRF Model Forecasts. [Available online at <http://www.nssl.noaa.gov/wrf>]

Ralph, F. M. and Coauthors, 2005: Improving Short-Term (0-48h) Cool-Season Quantitative Precipitation Forecasting. Recommendations from a USWRP Workshop. *Bull. Amer. Meteor. Soc.*, **86**, 1619-1632.

Skamarock, et al., cited 2007: A Description of the Advanced Research WRF Version 2. [Available online at <http://www.wrf-model.org/wrfadmin/publications.php>]

Stephens, G. L. and Coauthors, 2002: The CloudSat Mission and the A-Train. *Bull. Amer. Meteor. Soc.*, **83**, 1771-1790.

Syrett, W. J., B. A. Albrecht and E. E. Clothiaux, 1995: Vertical Structure in a Midlatitude Cyclone from a 94-GHz Radar. *Mon. Wea. Rev.*, **123**, 3393-3407.

Tao, W.-K. and Coauthors, 2007: Revised bulk-microphysical schemes for studying precipitation processes: Part I: Comparison with different microphysical schemes. *Mon. Wea. Rev.* (accepted with revision).

Wang, Z. and K. Sassen, 2001: Cloud Type and Macrophysical Property Retrieval Using Multiple Remote Sensors. *J. Appl. Met.*, **40**, 1665-1682.

Wang, Z. and K. Sassen, cited 2007: Level 2 Cloud Scenario Classification. Product Process Description and Interface Control Document. [Available online at <http://www.cloudsat.cira.colostate.edu/dataICDlist.php?go=list&path=/2B-CLDCLASS>]

Yuter, S. E. and R. A. Houze, 1995: Three-Dimensional Kinematic and Microphysical Evolution of Florida Cumulonimbus. Part II: Frequency Distributions of Vertical Velocity, Reflectivity, and Differential Reflectivity. *Mon. Wea. Rev.*, **123**, 1941-1963.